

Hoek-Brown parameters for predicting the depth of brittle failure around tunnels

C.D. Martin, P.K. Kaiser, D.R. McCreath

Abstract: A review of tunnels excavated in varying rock mass types and conditions, indicates that the initiation of brittle failure occurs when the damage index (D_i) expressed as the ratio of the maximum tangential boundary stress to the laboratory unconfined compressive strength exceeds ≈ 0.4 . When the damage index exceeds this value the depth of brittle failure around a tunnel can be estimated by using a strength envelope based solely on cohesion which in terms of the Hoek-Brown parameters implies that $m = 0$. It is proposed that in the brittle failure process peak cohesion and friction are not mobilized together, and that around underground openings the brittle failure process is dominated by a loss of the intrinsic cohesion of the rock mass such that the frictional strength component can be ignored for estimating the depth of brittle failure.

Case histories were analyzed using the Hoek-Brown failure criterion, with traditional frictional parameters and with the proposed brittle rock mass parameters: $m = 0$ and $s = 0.11$. The analyses show that use of a rock mass failure criteria with frictional parameters ($m > 0$) significantly underpredicts the depth of brittle failure while use of the brittle parameters provides good agreement with field observations. Analyses using the brittle parameters also show that in intermediate stress environments, where stress-induced brittle failure is localized, a tunnel with a flat roof is more stable than an tunnel with an arched roof. This is consistent with field observations. Hence, the Hoek-Brown brittle parameters can be used to estimate the depth of brittle failure around tunnels, the support demand-loads caused by stress-induced failure, and the optimum geometry of the opening.

Key words: spalling, depth of failure, rock mass strength, brittle failure criterion, cohesion loss, Hoek-Brown brittle parameters.

1 Introduction

Failure of underground openings in hard rocks is a function of the in-situ stress magnitudes and the characteristics of the rock mass, i.e., the intact rock strength and the fracture network (Fig. 1). At low in-situ stress magnitudes, the failure process is controlled by the continuity and distribution of the natural fractures in the rock mass. However as in-situ stress magnitudes increase, the failure process is dominated by new stress-induced fractures growing parallel to the excavation boundary. This fracturing is generally referred to as brittle failure. Initially, at intermediate depths, these failure regions are localized near the tunnel perimeter but at great depth the fracturing envelopes the whole boundary of the excavation (Fig. 1). Unlike ductile materials in which shear slip surfaces can form while continuity of material is maintained, brittle failure deals with materials for which continuity must first be disrupted before kinematically feasible failure mechanisms can form.

Attempts to predict either the onset of this brittle failure process or the maximum depth to which the brittle failure process will propagate, using traditional failure criteria based on frictional strength, have not met with much success (Wagner, 1987; Pelli et al., 1991; Martin, 1997; Castro et al., 1996; Grimstad and Bhasin, 1997).

One approach, which attempts to overcome this deficiency, is to model the failure process progressively by using iterative elastic analyses and conventional failure criteria. The initial zone of failure is removed, and the analysis is then repeated based on the updated tunnel geometry. This iterative process is intended to simulate the progressive nature of brittle failure. However, as noted by Martin (1997) this process is not self-stabilizing, and as a result over-predicts the depth of failure by a factor of 2 to 3.

Martin and Chandler (1994) demonstrated in laboratory experiments that in the brittle failure process peak cohesion and friction are not mobilized together and that most of the cohesion was lost before peak friction was mobilized. They postulated that around underground openings the brittle-failure process is dominated by a loss of the intrinsic cohesion of the rock mass such that the frictional strength component can be ignored. Recently, Martin (1997) showed that the maximum depth of stress-induced brittle fracturing around a circular test tunnel in massive granite could be approximated by a criterion that only considered the cohesive strength of the rock mass. This paper considers the applicability of this approach as a general criterion for estimating the depth of brittle failure around tunnels.

2 Rock mass strength around tunnels

The strength of a rock mass is often estimated by back-analyzing case histories where examples of failure have been carefully documented (Sakurai, 1993). In brittle rock masses

Accepted July 1998

C.D. Martin, P.K. Kaiser Geomechanics Research Centre, Laurentian University, Sudbury, ON, Canada P3E 2C6

D.R. McCreath School of Engineering, Laurentian University, Sudbury, ON, Canada P3E 2C6

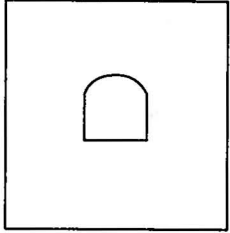
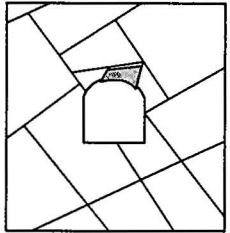
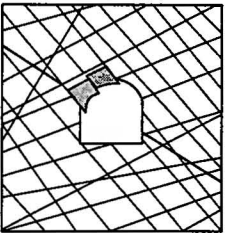
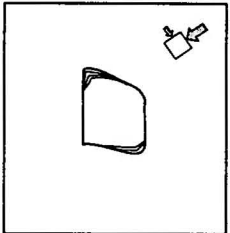
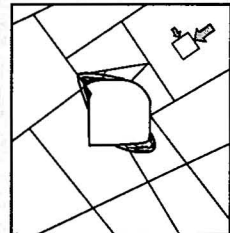
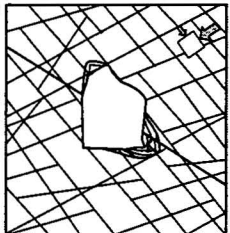
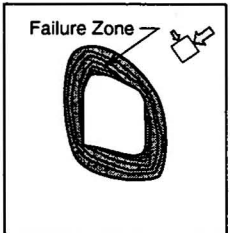
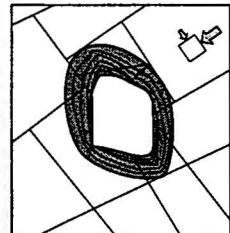
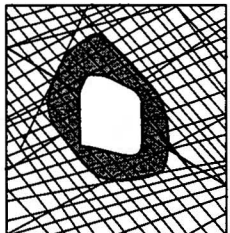
	Massive (RMR > 75)	Moderately Fractured (50 > RMR < 75)	Highly Fractured (RMR < 50)
Low In-Situ Stress ($\sigma_1 / \sigma_c < 0.15$)	 <p>Linear elastic response.</p>	 <p>Falling or sliding of blocks and wedges.</p>	 <p>Unravelling of blocks from the excavation surface.</p>
Intermediate In-Situ Stress ($0.15 > \sigma_1 / \sigma_c < 0.4$)	 <p>Brittle failure adjacent to excavation boundary.</p>	 <p>Localized brittle failure of intact rock and movement of blocks.</p>	 <p>Localized brittle failure of intact rock and unravelling along discontinuities.</p>
High In-Situ Stress ($\sigma_1 / \sigma_c > 0.4$)	 <p>Brittle failure around the excavation .</p>	 <p>Brittle failure of intact rock around the excavation and movement of blocks.</p>	 <p>Squeezing and swelling rocks. Elastic/plastic continuum.</p>

Fig. 1: Examples of tunnel instability and brittle failure (highlighted grey squares) as a function of Rock Mass Rating (RMR) and the ratio of the maximum far-field stress (σ_1) to the unconfined compressive strength (σ_c), modified from Hoek et al. (1995).

failure around tunnels occurs in the form of spalling or fracturing, and back analyses involve establishing the stresses required to cause this fracturing. Ortlepp et al. (1972) compiled experience from square 3-m to 4-m tunnels in brittle rocks in South African gold mines and suggested that the stability of these tunnels could be assessed using the ratio of the far-field maximum stress (σ_1) to the laboratory uniaxial compressive strength¹ σ_c :

$$[1] \quad \frac{\sigma_1}{\sigma_c}$$

¹The laboratory uniaxial compressive strength σ_c should be determined using the ISRM suggested methods for testing (Brown, 1981)

For a stress environment where the ratio of the maximum to minimum far-field stress (K_0) is equal to 0.5, they concluded that minor spalling occurs when $\sigma_1 / \sigma_c > 0.2$. Hoek and Brown (1980) compiled additional South African observations from underground mining in massive brittle rocks and suggested the stability classification given in Fig. 2. The stability classification in Fig. 2 ranges from 0.1 through 0.5 and can be briefly described as follows: ($\sigma_1 / \sigma_c \leq 0.1$) a stable unsupported opening, i.e., no damage; ($\sigma_1 / \sigma_c = 0.2$) minor spalling (failure) can be observed, requiring light support; ($\sigma_1 / \sigma_c = 0.3$) severe spalling (failure), requiring moderate support; ($\sigma_1 / \sigma_c = 0.4$) heavy support required to stabilize the

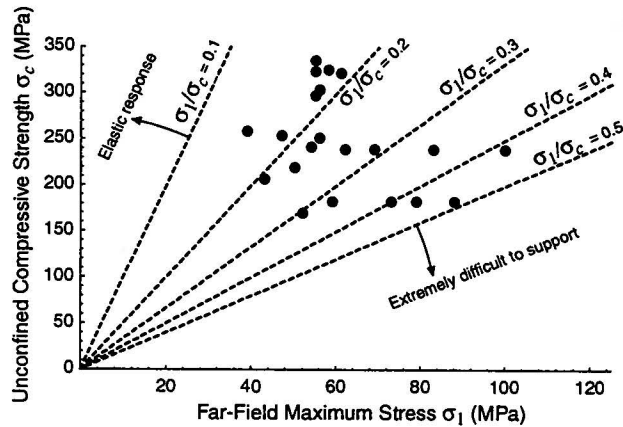


Fig. 2: Empirical stability classification developed for square tunnels in South Africa ($K_o = 0.5$), modified from Hoek and Brown (1980).

opening; and ($\sigma_1/\sigma_c = 0.5$) stability of the opening may be very difficult to achieve, extreme support required.

The stability classification developed by Hoek and Brown (1980) is not directly transferable to other tunnel shapes as it only considers the far-field stress under a constant $K_o = 0.5$. The stress-induced failure process initiates at the stress concentrations near the boundary of the tunnel and therefore the maximum tangential stress at the boundary of the tunnel, which is a function of tunnel shape, must be considered. Wiseman (1979) attempted to overcome this limitation by considering the stresses at the sidewall of the excavation. He proposed a sidewall stress concentration factor (SCF) given by:

$$[2] \quad SCF = \frac{3\sigma_1 - \sigma_3}{\sigma_c}$$

where σ_1 and σ_3 are the far-field in-situ stresses and σ_c is the laboratory uniaxial compressive strength. In a detailed survey of 20 km of gold mine tunnels Wiseman observed that the conditions for unsupported tunnels deteriorated rapidly when the sidewall stress concentration factor reached a value of about 0.8. Wiseman noted that the sidewall stress concentration factor provided the maximum tangential stress at the boundary of a circular opening but that none of the tunnels surveyed "was even approximately circular in cross section".

The South African examples illustrate that the stability of tunnels in massive rocks can be assessed by comparing stresses on the boundary of essentially square openings to the laboratory uniaxial compressive strength. However, to apply the South African empirical stability classification to other sites, the effect of the tunnel geometry and varying stress ratios on the maximum tangential stress at the boundary of the tunnel must be evaluated. Numerical programs can readily be used to assess these effects on the boundary stress. Alternatively the closed form solution developed by Greenspan (1944) can be used for tunnel geometries that can be expressed in the parametric form given by:

$$[3] \quad x = p \cos \beta + r \cos 3\beta, \quad y = q \sin \beta - r \sin 3\beta$$

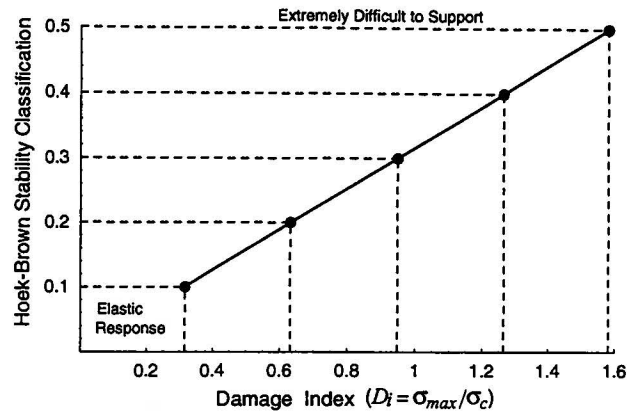


Fig. 3: Damage index expressed as a function of the ratio of σ_{max} to σ_c for the stability classifications given in Fig. 2.

where p, q and r are parameters and β is an angle. Through the appropriate choice of p, q and r , near-rectangular openings can be analyzed and this approach has been used to determine the maximum tangential stress for the case histories used by Hoek and Brown (1980).

The conversion of the classification expressed in Fig. 2 into terms which consider the maximum tangential boundary stress (σ_{max}) is given in Fig. 3. The ratio of σ_{max} to the laboratory short-term unconfined compressive strength (σ_c) will be referred to as the damage index (D_i). The damage index indicates that for $D_i \leq 0.4$ the rock mass is basically elastic and no visible damage is recorded. Hence the maximum rock mass strength near the opening, in the case histories used by Hoek and Brown (1980), is approximately $0.4\sigma_c$. This notion that the field strength of massive or moderately jointed rock is approximately one half the laboratory strength has been reported by several researchers for a wide range of rock types (e.g. see Martin, 1995; Pelli et al., 1991; Myrvang, 1991; Stacey, 1981).

The shear strength of a rock mass is usually described by a Coulomb criteria with two strength components: a constant cohesion and a normal-stress dependent friction component. In 1980, Hoek and Brown, proposed an empirical failure criterion which is now widely used in rock engineering and in the generalized form is given as:

$$[4] \quad \sigma'_1 = \sigma'_3 + \sigma_c \left(m \frac{\sigma'_3}{\sigma_c} + s \right)^a$$

where σ'_1 and σ'_3 are the maximum and minimum effective stresses at failure, σ_c is the laboratory uniaxial compressive strength, and the empirical constants m and s are based on the rock mass quality. For most hard-rock masses the constant a is equal to 0.5 and Equation 4 is usually expressed in the following form:

$$[5] \quad \sigma_1 = \sigma_3 + \sqrt{m\sigma_c\sigma_3 + s\sigma_c^2}$$

where σ_1 and σ_3 are again the maximum and minimum effective stresses at failure. The empirical constants are related

in a general sense to the angle of internal friction of the rock mass (m) and the rock mass cohesive strength (s) and Hoek and Brown (1980) provided a methodology for deriving the frictional and cohesive strength components for a given normal stress. For both the Coulomb or the Hoek-Brown failure criteria, it is implicitly assumed that the cohesive (c or s) and the frictional (ϕ or m) strength components are mobilized simultaneously.

Hoek and Brown (1980) suggested that m and s can be estimated by:

$$[6] \quad m = m_i \exp\left(\frac{\text{RMR} - 100}{28}\right)$$

and

$$[7] \quad s = \exp\left(\frac{\text{RMR} - 100}{9}\right)$$

where m_i is the value of m for intact rock and RMR is the rock mass rating based on the classification system developed by Bieniawski (1989). It can be seen from Equations 6 and 7 that as the rock mass quality improves, i.e., RMR approaches 100, the strength of the rock mass approaches the strength of the intact rock. For the boundary of a tunnel, where $\sigma_3 = 0$, Equation 5 reduces to:

$$[8] \quad \sigma_1 = \sqrt{s\sigma_c^2}$$

and for intact rock $s = 1$ such that at the boundary of a tunnel when failure occurs σ_1 should be approximately equal to σ_c . However, Read and Martin (1996) has shown, from recent experience with the Mine-by test tunnel in massive intact granite (RMR ≈ 100), that for even these conditions where the rock mass is intact s is approximately equal to 0.25 such that $\sigma_1 \approx 0.5\sigma_c$. This is in keeping with the South African experience described previously, where failure on the boundary of tunnels initiates at about $0.4\sigma_c$ or in terms of the Hoek-Brown parameter $s = 0.2$. Martin (1997) attributed this difference between the laboratory strength and in-situ strength to the loading path. In the laboratory the strength is estimated via a simple monotonically increasing loading path where as the in-situ strength is mobilized essentially by unloading the rock mass through a complex loading path involving stress rotation. Hence, it would appear that the strength in-situ can only be estimated by back-analyses and that for tunnels in massive rocks the in-situ rock mass strength is approximately $0.4\sigma_c$. While this approach is useful to establish the rock mass strength at zero confining stress, it cannot be used to estimate the depth of failure, an essential parameter in designing the rock support for these tunnels. This aspect of brittle failure is discussed in the following sections.

3 Characteristics of stress-induced brittle failure

A characteristic of stress-induced failure of tunnels in brittle rock is the notched-shape of the failure region and the associated slabbing and spalling which may occur in a stable manner

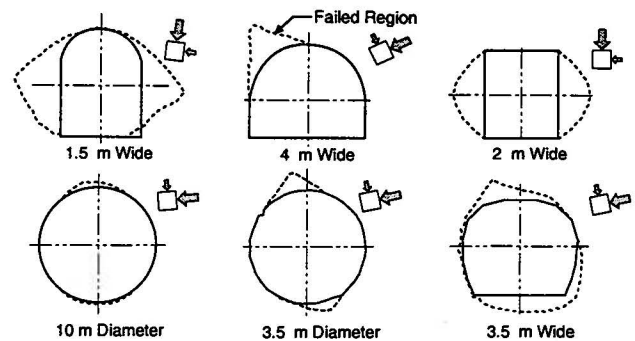


Fig. 4: Comparison of the failed (notch) region for tunnels of different size and shape. The orientation of the maximum and minimum in-situ stresses, in the plane of the excavation, is shown.

or violently in the form of strainbursts. These slabs can range in thickness from a few millimetres to tens of centimetres and with large openings can be several square metres in surface area (see Ortlepp, 1997; Martin et al., 1997). Fairhurst and Cook (1966) suggested that the formation and thickness of these slabs could be related to strain energy. Martin et al. (1997) provided detailed observations of the failure process around a circular test tunnel and concluded that the slab formation is associated with the advancing tunnel face, and that once plane-strain conditions are reached the new notched-tunnel shape is essentially stable. More importantly, their observations showed that the brittle failure process forms slabs which have very little cohesive strength between the slabs such that when subjected to gravitational loading they fall from the roof. Yet outside this notch region they found that the rock mass was much less damaged and retained its integrity. For support design purposes this observation is extremely important as only the rock mass slabs inside the failure region needs to be supported and the extent or depth of the failure zone determines the required bolt length.

A review of published case histories where the shape of the slabbing region has been measured and documented, shows that the brittle failure process leads to the development of a v-shaped notch, regardless of the original opening shape or size (Fig. 4). As shown in Fig. 4 the location, extent and depth of the notch, and hence the support requirements, can vary significantly.

In the previous section it was shown that the formation of the notch initiates when the tangential stresses on the boundary of the tunnel exceed approximately $0.4\sigma_c$. At these stress levels the failure process involves micro-scale fracturing that can be detected with microseismic monitoring equipment (Martin et al., 1995). Observations from around tunnels indicates that these micro-scale fractures lead to the formation of slabs that grow in a plane parallel to the tunnel boundary, i.e., normal to σ_3 , such that the mode of origin of these macro-scale fractures is extension.

An earlier attempt to predict the depth of brittle failure around tunnels in massive quartzites was carried out by Stacey (1981). He proposed that the on-set and depth of failure could be estimated by a considering the extension strain which can

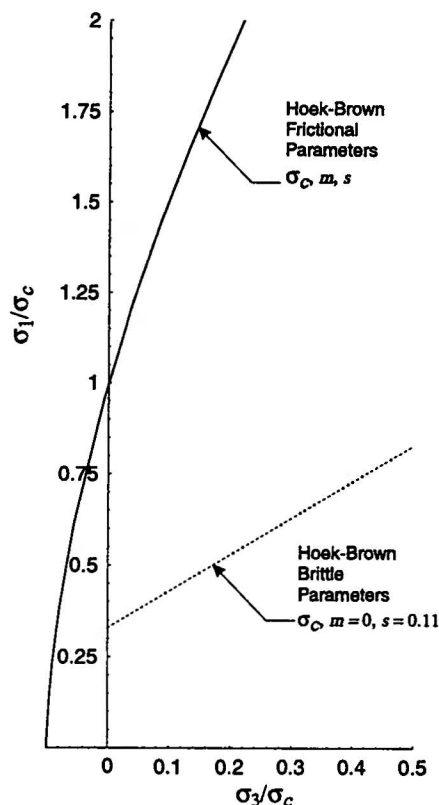


Fig. 5: Illustration of the Hoek-Brown envelope for frictional (σ_c, m, s) and brittle ($\sigma_c, m = 0, s = 0.11$) parameters.

be calculated from:

$$[9] \quad \epsilon = \frac{1}{E} [\sigma_3 - \nu(\sigma_1 + \sigma_2)]$$

where ν is the Poisson's ratio and E is the Young's modulus of the rock mass. Stacey (1981) proposed that if the calculated extension strain was greater than the critical extension strain, spalling would occur. The notion that an extensional strain criterion could be used to predict the depth of spalling coupled with the observational evidence that the spalling process involves the growth of extension-like fractures around tunnel suggests that the brittle failure process is controlled by the cohesion of the rock mass. Stacey and Page (1986) suggests that where the failure is non-brittle a more appropriate criterion to apply is that based on a shear failure mechanism.

More recently, Martin and Chandler (1994) showed via damage-controlled laboratory tests that the accumulation of these extension cracks reduces the intrinsic cohesion of the intact rock and that this reduction in cohesion occurs before the peak strength of the sample is reached. While it is customary to assume that the peak friction and peak cohesion of a rock mass are mobilized at the same displacements, their results showed that cohesion is reduced by about 70% as friction is fully mobilized and that this reduction occurs after only a small amount of damage or inelastic straining. Martin (1997)

also showed, based on microseismic evidence, that damage-initiation and the depth of failure around the Mine-by test tunnel could be approximated by a constant deviatoric stress; $\sigma_1 - \sigma_3 = 75 \text{ MPa}$ or $1/3\sigma_c$. Other researchers, (e.g., Brace et al., 1966; Scholz, 1968; Peng and Johnson, 1972; Hallbauer et al., 1973; Martin and Chandler, 1994), have also found that the initiation of fracturing in uniaxial laboratory tests occurs between 0.25 and $0.5\sigma_c$ for a wide variety of rock types and concrete. The constant deviatoric stress Equation proposed by Martin can be expressed in terms of the Hoek-Brown parameters as:

$$[10] \quad \sigma_1 = \sigma_3 + \sqrt{3s\sigma_c^2}$$

by setting the frictional constant m to zero to reflect that the frictional strength component has not been mobilized and $\sqrt{s} = 1/3$ (Fig. 5). Implicit in Equation 10 is the notion that the stress-induced brittle failure process, that occurs around tunnels, is dominated by cohesion loss caused by the growth of extension cracks near the excavation boundary. Stacey (1981) conducted laboratory tests and found that for most brittle rocks the critical strain for extension fracturing was only slightly dependent on confining stress and occurred in the region of $0.3\sigma_c$. Hence, Stacey's extension strain criterion is based on the same mechanistic model as Equation 10. In other words the critical strain criterion corresponds to the proposed "cohesion loss before friction mobilization" model.

It is important to note that Equation 10 is only applicable when considering stress-induced brittle failure. It cannot be used to define regions of tensile failure as it overestimates the tensile strength of the rock mass. If tensile failure is of concern, a Mohr-Coulomb criterion with a tension cut-off would be more appropriate. In the next section Equation 10, which was developed for the Mine-by test tunnel in massive granite, is applied to other rock masses.

4 Depth of stress-induced failure

The failure zone that forms around an underground opening is a function of the geometry of the opening, the far-field stresses and the strength of the rock mass. Detournay and St. John (1988) categorized possible failure modes around a circular unsupported tunnel according to Fig. 6. The mean and deviatoric stress in Fig. 6 is normalized to the uniaxial compressive field strength (σ_c^*) which is assumed to be approximately $0.5\sigma_c$ for the data superimposed on Fig. 6. In Region I, the extent of the predicted failure zone is localized, and only at large values of the deviatoric and/or mean stress does the failure shape become continuous.

The shape of the region defined by Equation 10 is controlled by the ratio (K_o) of the maximum stress to minimum stress (σ_1/σ_3) in the plane of the tunnel cross section. For a $K_o = 1$ damage should theoretically occur uniformly around a circular tunnel when the normalized mean stress exceeds 0.5. However, practical experience indicates that due to heterogeneities, failure is always localized. Fig. 7 illustrates the effect of K_o on the shape of the region defined by Equation 10. As K_o increases,

Table 1: Summary of case histories used to establish relationship between depth of failure and maximum tangential stress. All tunnels are circular except where noted.

Rock Mass	R_f/a	σ_1/σ_3	σ_3 (MPa)	σ_c (MPa)	Reference
Blocky andesite ^a	1.3	1.92	15.3	100	GRC field notes (El Teniente Mine)
	1.5	2.07	14.8	100	
	1.4	2.03	14.7	100	
	1.5	2.10	16.3	100	
	1.5	2.03	15.4	100	
Massive quartzites ^a	1.6	2.09	15.8	100	Ortlepp and Gay (1984)
	1.8	2.15	65	350	
	1.7	2.15	65	350	
	1.4	1.86	60	350	
	1.5	1.86	60	350	
Bedded quartzites	1.4	3.39	15.5	250	Stacey and de Jongh (1977)
	1.3	3.39	15.5	250	
Massive granite	1.5	5.36	11	220	Martin et al. (1994)
	1.4	5.36	11	220	
	1.4	5.36	11	220	
	1.3	5.36	11	220	
	1.3	5.36	11	220	
Massive granite	1.0	3.7	11	220	Martin (1989)
	1.1	1.31	40	220	
Interbedded siltstone-mudstone	1.4	2.0	5	36	Pelli et al. (1991)
Bedded limestone	1.1	1.3	12.1	80	Jiayou et al. (1989)
Bedded quartzites	1.0	1.69	21	217	Kirsten and Klokow (1979)
	1.08	1.69	20	151	

^aD-Shaped Tunnel

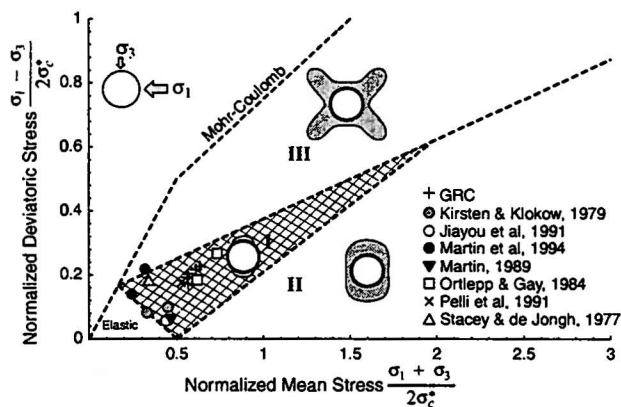


Fig. 6: Relationship between failure modes and far-field stress state for an unsupported circular opening, after Detournay and St. John (1988).

the shape of the damage region approaches that described as Region III in Fig. 6. However, the notch shapes presented in Fig. 4 do not match the shape of the damaged regions presented in Fig. 7. Equation 10 only describes the locus of damage initiation, and does not describe the limit of damage evolution, i.e., the extent of the slabbing process. Equation 10 therefore, pro-

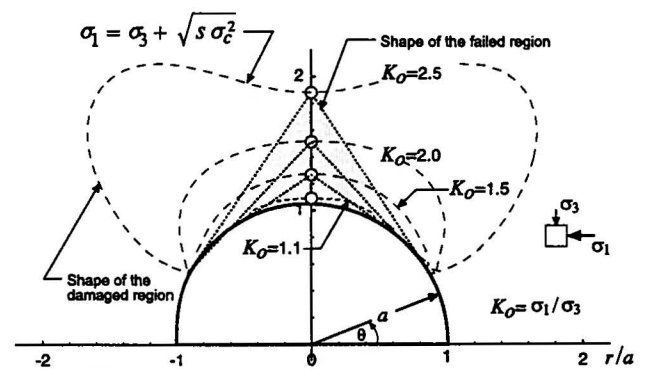


Fig. 7: Extent of damage around a circular opening defined by Equation 10, for various K_o ratios.

vides an estimate of the limiting depth to which slabbing can propagate but not of the shape of the slabbing region. Because of the progressive nature of this slabbing process, driven by the gradual stress increase associated with tunnel advance, the notch starts to propagate from the point of maximum tangential stress (in the roof at $\theta = 90^\circ$ in Fig. 7) towards the damage initiation limit described by Equation 10. It propagates until it reaches the deepest point of damage in the direction of the minor principal stress (circles in Fig. 7). If this is the case, then

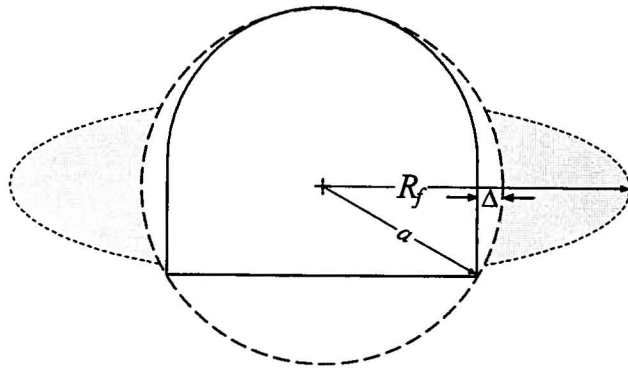


Fig. 8: Illustration of the D-shaped tunnel with an effective tunnel radius and the depth of failure (R_f).

the depth of failure should be predictable by using Equation 10.

A review of available literature identified 8 case histories where the depth and shape of failure around individual tunnels had been measured (Table 1). These case histories also provided a description of the rock type, σ_c , and the in-situ stress state. Examples of the reported notch shapes are shown in Fig. 4 and these case histories are also plotted in Fig. 6. They represent a wide range of stress, rock mass conditions and tunnel geometries, yet in all cases a well developed notch formed. Region II, involving yielding or squeezing ground conditions, are typically encountered in rock masses that are relatively weak compared to the mean stress or at great depth in hard rock.

The tunnels listed in Table 1 have either a circular cross section or a D-shaped section. Where the tunnels are D-shaped, an effective tunnel radius is used, as illustrated in Fig. 8. The depth to which the notch propagated in the case histories, is plotted in dimensionless form in Fig. 9. This depth of failure (R_f) in Fig. 9 has been normalized to either the tunnel radius or effective tunnel radius, and the maximum tangential stress (σ_{max}) has been normalized to σ_c . Where the tunnel is D-shaped, the distance from the wall to the equivalent circular shape (Δ in Fig. 8) is not included in the depth of the notch. The data suggest that the depth of failure can be approximated by a linear relationship given as:

$$[11] \quad \frac{R_f}{a} = 0.49(\pm 0.1) + 1.25 \frac{\sigma_{max}}{\sigma_c}$$

where $\sigma_{max} = 3\sigma_1 - \sigma_3$ and that failure initiates when $\sigma_{max}/\sigma_c \approx 0.4 \pm 0.1$. This initiation of failure is in good agreement with the findings discussed previously in Fig. 3.

Fig. 10 shows the predicted depth of failure, using Equation 10, with $s = 0.11$ as the criteria for the initiation of damage. This results in a slight over-prediction of the normalized depth of failure in Fig. 10 for σ_{max}/σ_c between 0.34 and 0.6. However, the prediction shows a similar linear trend as that measured for the range of damage indexes considered.

The concept of using the Hoek-Brown brittle parameters to define the damaged region around an underground opening was developed for massive unfractured granite (Martin, 1995). The

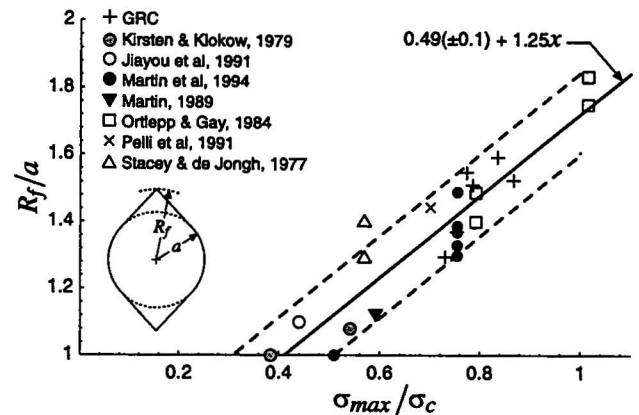


Fig. 9: Relationship between depth of failure and the maximum tangential stress at the boundary of the opening.

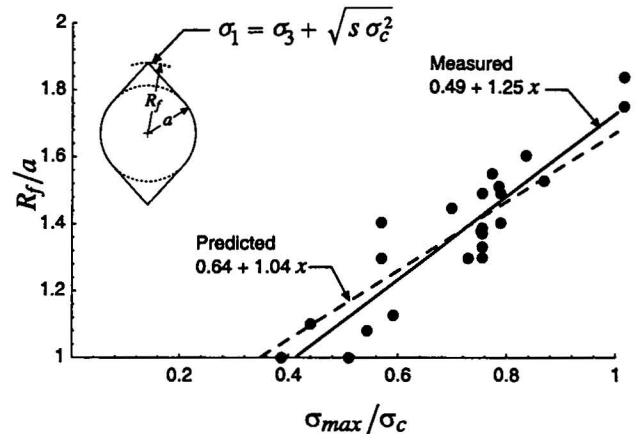


Fig. 10: Comparison between the predicted depth of damage initiation using the Hoek-Brown brittle parameters given by Equation 10 and measured depths of failure given in Table 1.

results presented in Fig. 10 suggest that the Hoek-Brown brittle parameters is applicable to a much wider range of rock mass types, e.g., interbedded mudstones and siltstones through to massive quartzites. The common elements in these case studies are that failure is stress-induced, the rock mass is moderately jointed to massive, and the rock mass behaviour is brittle. In these cases the discontinuities in the rock mass are not persistent relative to the size of the opening such that the failure process is essentially one of cohesion loss. In the next section the Hoek-Brown brittle parameters are applied to several well documented case histories and is also used to assess the effect of tunnel geometry on the depth of brittle failure.

5 Application of Hoek-Brown brittle parameters

In the previous section most of the analyses, using Hoek-Brown brittle parameters, were applied to near circular openings in fairly massive rocks. In this section the same concepts are

applied to other opening shapes and to rock masses that are described as anisotropic. All analyses in this section were carried out using the elastic boundary element program Examine2D (Curran and Corkum, 1995) or the plastic-finite element program Phase2 (Curran and Corkum, 1997). In these programs the stability is expressed in terms of a Strength Factor which is analogous to the traditional factor of safety such that a Strength Factor <1 implies failure or the region that is overstressed.

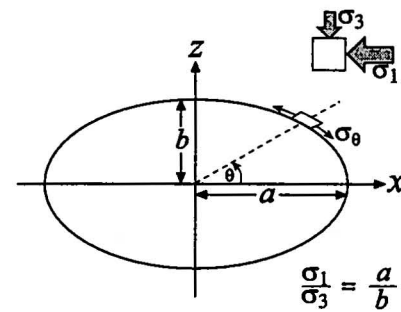
Martin (1997) showed the brittle failure process initiates near the tunnels face and hence is three-dimensional. Thus it is not surprising, as indicated by Fig. 7, that two-dimensional analyses using the Hoek-Brown brittle parameters cannot be used to predict the actual shape of the notch. Nonetheless, for the support design purposes it is necessary to determine how deep failure will occur and the lateral extent of failure. This can be achieved by the application of the Hoek-Brown brittle parameters. In the following example applications, taken from documented case histories, a comparison of the results with both Hoek-Brown frictional and brittle parameters are presented to demonstrate that this approach can be used to estimate the depth of failure.

5.1 Elastic versus plastic analyses

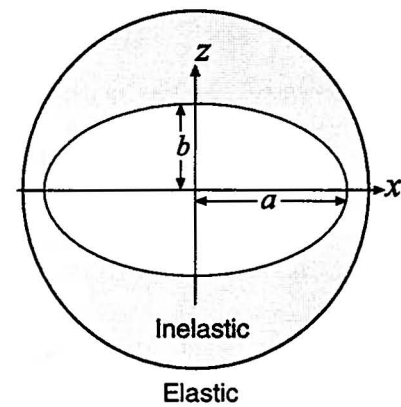
The theory of elasticity would suggest that the optimum shape of a tunnel is an ellipse with the major axis parallel to the direction of maximum in-plane stress, with the ratio of major (2a) to the minor (2b) axis of the ellipse being equal to the ratio of the maximum (σ_1) to minimum (σ_3) stresses in the plane of the excavation (Fig. 11a). This optimum shape produces uniform tangential stresses on the boundary of the excavation with the tangential stress equal to $\sigma_1 + \sigma_3$. Fairhurst (1993) pointed out however, that while the tangential stress is constant on the boundary it is not constant for the regions behind the boundary of the tunnel and should failure occur the inelastic region that develops for an elliptical shaped tunnel, is much larger than if the tunnel geometry were circular or an ellipse oriented parallel to the minimum stress axis (Fig. 11b).

Read and Chandler (1997) carried out an extensive study to evaluate the effect of tunnel shape on stability by excavating a series of ovaloid and circular openings at the Underground Research Laboratory, Manitoba. Because of the extreme in-situ stress ratio ($K_o \approx 6$) it was not practical to excavate an ellipse of the optimum shape (e.g, 18 m by 3 m in dimension). As a compromise, they excavated an ovaloid 6.6 m wide and 3 m high in a rock mass with the following average properties:

Rock Type	Granite	
In-situ stress	σ_1, σ_3	59.6, 11.1 MPa
Intact rock strength	σ_c	224 MPa
Rock Mass Rating	RMR	≈ 100
Hoek-Brown constants	m	28
	s	0.16
Residual parameters	m_r	1
	s_r	0.01



(a) Definitions

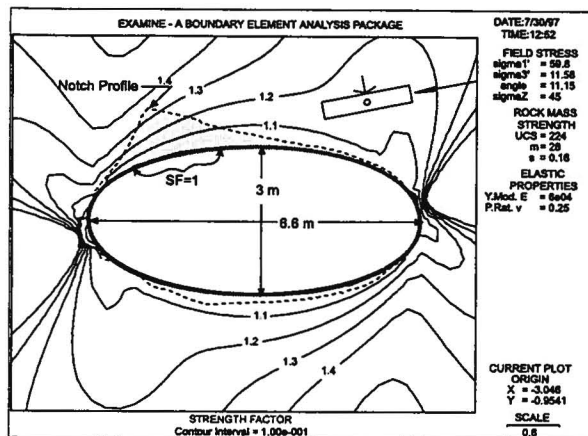


(b) Failure around an ellipse

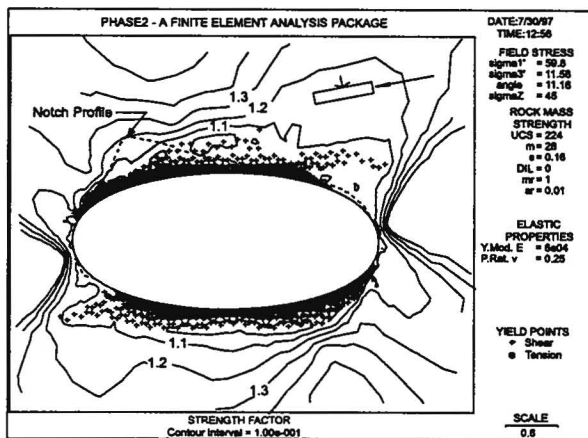
Fig. 11: Illustration of the stress distribution and inelastic zone for an elliptical tunnel, modified from Fairhurst (1993).

Fig. 12 shows the results from two analyses using Examine2D and the shape of the notched region that formed shortly after excavation (Read, pers. comm.). In the first analyses, the Hoek-Brown parameters are based on laboratory strength tests which gave $\sigma_c = 224$ MPa and $m = 28$, but with the parameter $s = 0.16$ to reflect that failure initiates at about $0.4\sigma_c$, consistent with the findings in Section 2. Those results are shown in Fig. 12a and indicate that the excavation is stable, i.e., the Strength Factor > 1, except for a very thin (approximately 50 mm thick) zone.

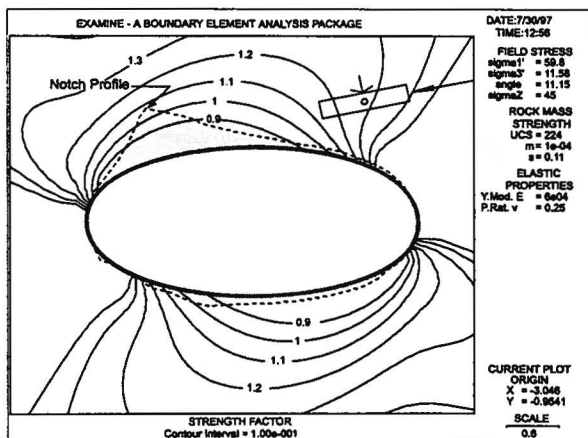
One of the limitations of the two-dimensional elastic analyses is that it does not account for the effect of stress redistribution as failure progresses. Hoek et al. (1995) suggested that elastic-brittle-plastic analyses are adequate for most practical purposes. They indicated that in order to simulate the elastic-brittle-plastic failure process in Lac du Bonnet granite, the Hoek-Brown residual parameters should be assigned very low values, e.g., $m_r = 1$ and $s_r = .01$ to simulate brittle failure. Fig. 12b shows the results from the plastic-finite-element program Phase2 with the parameters noted above. In this case failure is indicated as shown by the yield points in Fig. 12b.



(a) Elastic analysis with Hoek-Brown frictional parameters



(b) Elastic-brittle-plastic analysis



(c) Elastic analysis with Hoek-Brown brittle parameters

Fig. 12: Stability of a near-elliptical-shaped opening.

However, the location and depth of the notch is not captured by this approach and the results are very sensitive to the values for m_r and s_r which are difficult to determine.

The elastic analysis was repeated with the Hoek-Brown brittle parameters ($m = 0$ and $s = 0.11$) to estimate the depth of failure. Fig. 12c shows that this approach indicates that failure will occur but unlike the elastic-brittle-plastic analyses it more accurately predicts the maximum depth of failure. Most interestingly, this analysis also provides a good estimate of the extent of failure, encompassing nearly the entire roof of the excavation. This is consistent with field observations where Read (pers. comm.) reported that the slabs several centimetres thick formed over the width of the long side of the notch.

The case history in this section serves to illustrate that elastic analyses combined with the appropriate Hoek-Brown brittle parameters are adequate for practical purposes to estimate the depth and extent of the stress-induced failure zone in massive rocks. In the next sections this approach is used to analyze tunnels in moderately fractured anisotropic rocks.

5.2 Anisotropic rock masses

5.2.1 Weak Sedimentary rock mass

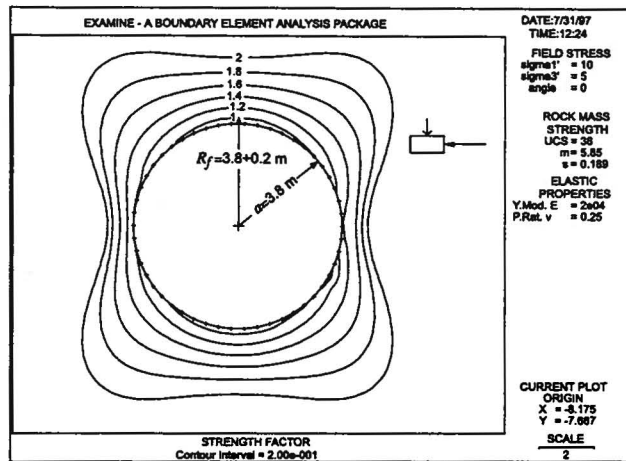
The following case study is taken from the construction of the Donkin-Morien tunnel and reported by Pelli et al. (1991). The 3.8-m-radius tunnel was excavated using a tunnel boring machine in a Sedimentary rock mass with the following average properties:

Rock Type	Interbedded Siltstone-mudstone
In-situ stress	σ_1, σ_3 10, 5 MPa
Intact rock strength	σ_c 36 MPa
Rock Mass Rating	RMR 85
Hoek-Brown constants	m 5.85
	s 0.189

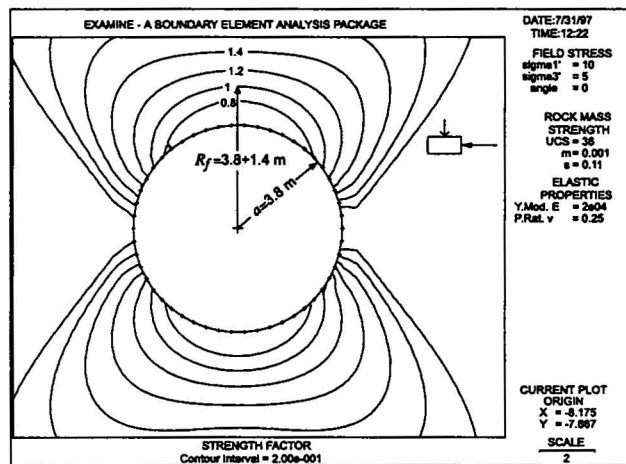
Pelli et al. (1991) reported that the depth of 'loosening' of the rock mass in the crown of the tunnel extended to between 1 and 1.4 m. Fig. 13a shows the results from the elastic analyses using the Hoek-Brown parameters recommended for the rock mass conditions. While failure of the crown is indicated in Fig. 13a it is considerably less than measured in the field. Pelli et al. (1991) conducted parametric analyses and concluded that the range of Hoek-Brown parameters that matched field observations were clearly outside the range recommended by Hoek and Brown (1988) for this quality rock mass and suggested that much lower m and higher s values would provide a better fit. Fig. 13b shows the results from the analyses with $m = 0$ and $s = 0.11$. For these parameters the depth of failure is in much better agreement with the measured failure.

5.2.2 Foliated rock mass

In the previous examples, the failure occurred during or shortly after excavation. In this example reported by Nickson et al. (1997), failure around an existing shaft occurred after adjacent mining caused elevated stresses in the vicinity of the excavation



(a) Hoek-Brown frictional parameters



(b) Hoek-Brown brittle parameters

Fig. 13: Depth of failure of a 3.8-m-radius tunnel excavated in weak sedimentary rocks.

The 4 m by 6 m shaft was excavated in foliated rock mass with the following average properties:

Rock Type	Metasediments
In-situ stress	σ_1, σ_3 35, 23.4 MPa
Intact rock strength	σ_c 100 MPa
Rock Mass Rating	RMR 66
Hoek-Brown constant	m 5.2
	s 0

Nickson et al. (1997) carried out a detailed assessment of the damage to the shaft and noted the following (Fig. 14): (1) the rock in the two opposite corners of the shaft was extensively crushed while the other corners showed only minor crushing; (2) the east and west walls of the shaft extensively spalled with the maximum depth of failure in the east wall extending to ap-

proximately 2 m and the depth of failure in the west wall being somewhat less; and (3) no evidence of spalling was observed on the north and south walls of the shaft.

Nickson et al. (1997) carried out extensive three dimensional numerical analyses to determine the in-situ failure envelope needed to match the observed damage around the shaft. They concluded that the slope of the failure line in σ_1/σ_3 space was slightly less than 1, which implies that $m \approx 0$.

Two dimensional elastic analyses were carried out to determine whether the Hoek-Brown brittle parameters could capture some of the reported observations. Fig. 14a shows that the traditional Hoek-Brown parameters for this rock mass would indicate failure of the North and South walls with little failure at the Northeast and Southwest corners. This is clearly inconsistent with observations. However, the results from the analysis using the Hoek-Brown brittle parameters presented in Fig. 14b are in good agreement with the observations noted by Nickson et al. (1997). In particular, the maximum depth of failure of the East wall, reported as 2 m, corresponds well with the predicted depth of 2.2 m. Interestingly, the Hoek-Brown brittle parameters predicted the non-symmetric crushing at the two corners which also agrees well with observations.

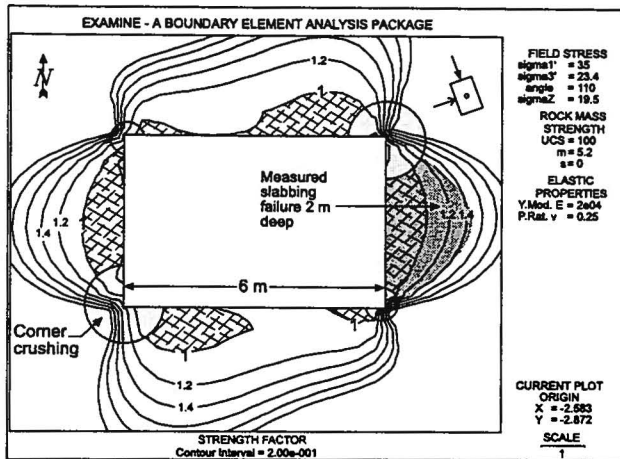
5.3 Depth of failure and tunnel shape

The stress distribution around an excavation in an elastic rock mass is controlled by the shape of the excavation. For example, openings with corners or small radii of curvature will have high compressive stress concentrations in these locations. Hence, there is a tendency to increase the radius of curvature in the design of underground openings, to avoid overstressing of the rock mass. This is particularly evident in civil engineering where tunnels are frequently circular or horse-shoe shaped. In mining, development tunnels often have rectangular shapes with a slightly arched roof to also reduce stress concentrations. However, mining experience suggests that in intermediate-stress environments rectangular-shaped openings with arched roofs (Castro and McCreath, 1997). In the following, the Hoek-Brown frictional and brittle parameters are used to evaluate the stability of tunnels with both arched and flat roofs.

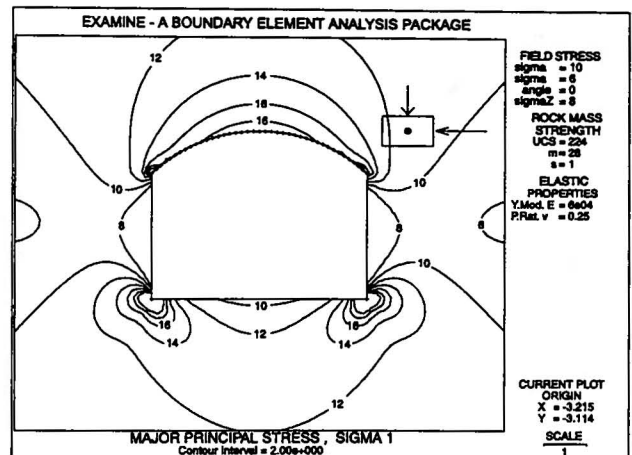
5.3.1 Arched roof: Low in-situ stress

In low-stress environments in the Canadian Shield (to approximately 250 m depth) the rock mass response tends to be elastic as the Damage Index is less than 0.4, and hence stability is controlled by the rock mass structure (see Figs. 1 and 2). Thus the optimum tunnel geometry should reduce the possibility of blocks falling from the roof. Brady and Brown (1993) have shown that sliding along a plane from the roof of a tunnel can be evaluated in two dimensions by:

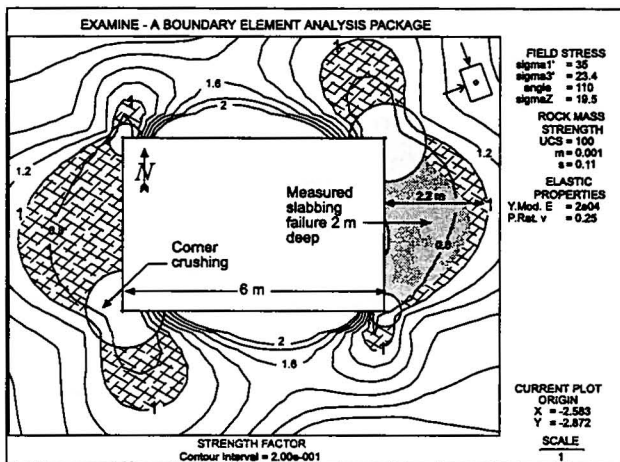
$$[12] \quad \sigma_{1f} = \frac{2c + \sigma_3 [\sin 2\beta + \tan \phi(1 - \cos 2\beta)]}{\sin 2\beta - \tan \phi(1 + \cos 2\beta)}$$



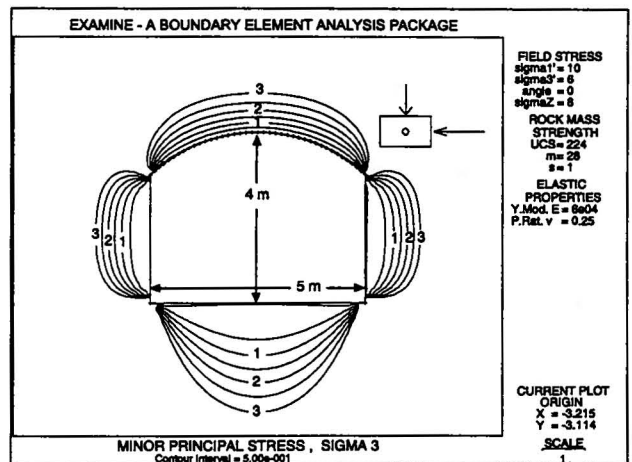
(a) Hoek-Brown frictional parameters



(a) Sigma 1



(b) Hoek-Brown brittle parameters



(b) Sigma 3

Fig. 14: Depth of failure of around shaft excavated in a foliated rock mass.

Fig. 15: Principal stresses around a tunnel with an arched roof in a rock mass with low in-situ stresses.

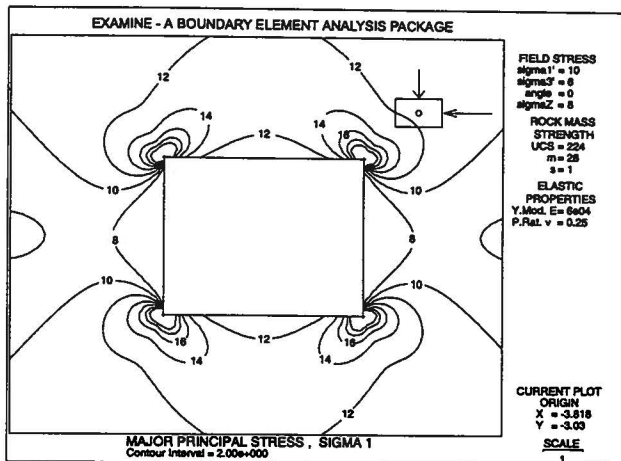
where σ_3 is the minimum principal stress in the plane, c is the cohesive strength, ϕ is the friction angle and β is the angle of the failure plane relative to σ_3 .

Equation 12 illustrates that the confining stress σ_3 plays a major role in structurally-controlled stability. Hence, an optimum tunnel geometry should reduce the region of low σ_3 close to the tunnel roof. Figs. 15 and 16 show the elastic principal stresses around a typical mine development tunnel with an arched and flat roof. Comparing Figs. 15 and 16, it is immediately evident that a flat roof causes a much bigger region of unloading, i.e., low σ_3 , and hence would promote structural failure. Thus in a low stress environment, an arched roof is a better choice in minimizing the potential for structurally-controlled failure.

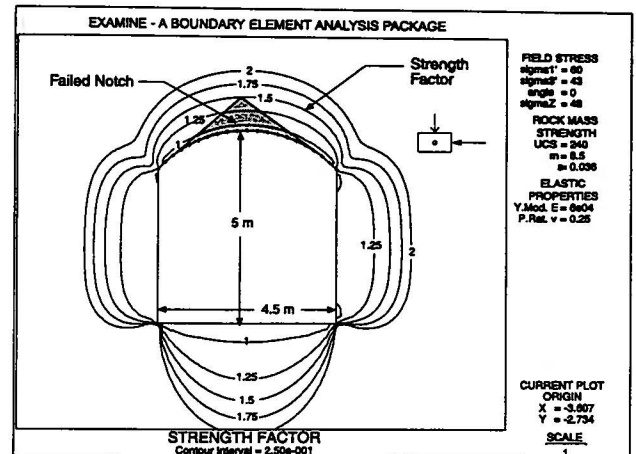
5.3.2 Arched roof: Intermediate in-situ stress

In an intermediate-stress environment in the Canadian Shield (approximately to 1500 m depth) the rock mass response is non-elastic as $D_i > 0.4$, and hence stability is controlled by the stress-induced damage in the roof (see Figs. 1 and 2). In order to optimize the tunnel shape in this stress environment, a failure criterion is required that adequately predicts the zone of failure. To evaluate whether a frictional-based failure criterion is appropriate for predicting the depth of stress-induced failure a case history is analyzed from a Canadian mine (S. Easley, pers. comm.).

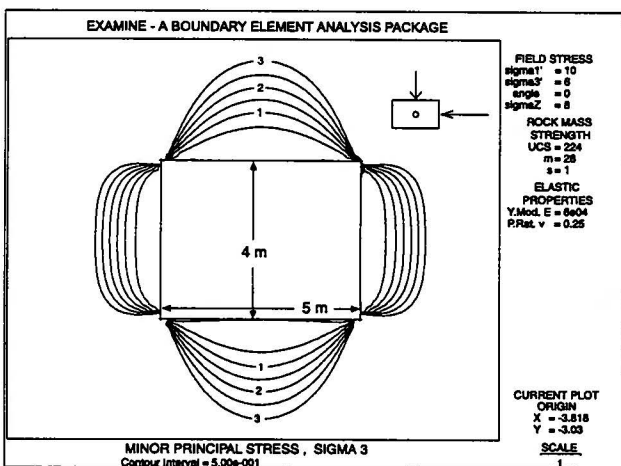
A 4.5 m wide and 5 m high tunnel, with an arched roof, was excavated in a moderately jointed rock mass with the following average properties:



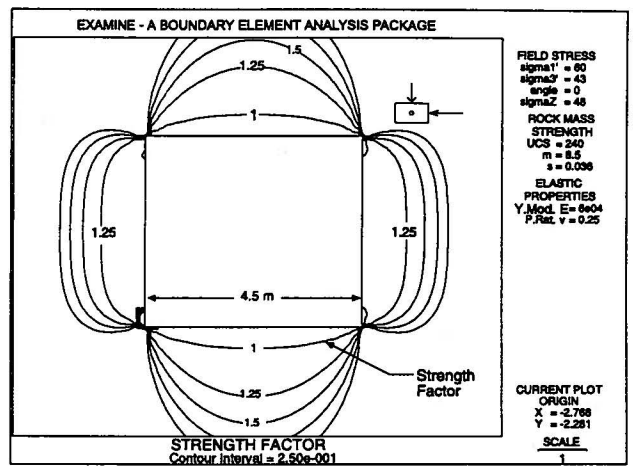
(a) Sigma 1



(a) Arched roof



(b) Sigma 3



(b) Flat roof

Fig. 16: Principal stresses around a tunnel with a flat roof in a rock mass with low in-situ stresses.

Fig. 17: Depth of failure using Hoek-Brown frictional parameters for a tunnel with a flat-roof and an arched roof.

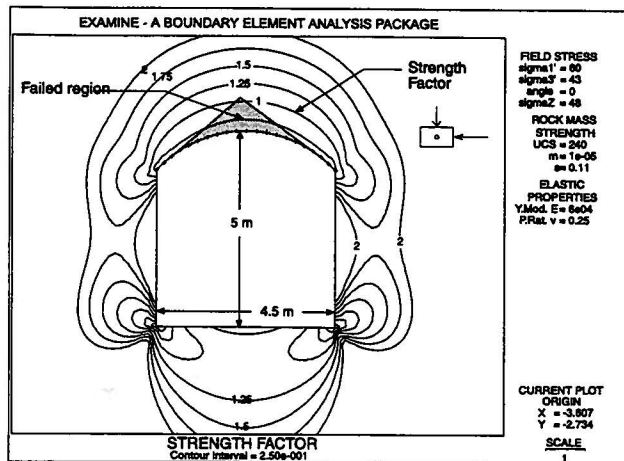
Rock Type	Granite gneiss
In-situ stress	σ_1, σ_3 60, 43 MPa
Intact rock strength	σ_c 240 MPa
Rock Mass Rating	RMR 70
Hoek-Brown constants	m 8.5
	s 0.036

Failure of the roof progressed during excavation of the tunnel to form a v-shaped notch to a depth of approximately 1 m, similar to that shown in Fig. 17. The tunnel roof geometry was changed from the 1-m-high arch to a flat roof. This change in geometry prevented the development of the notch in the flat roof and allowed the tunnel to be excavated with standard roof bolting. To determine if this change in geometry was the main reason for the rock mass response, the arched tunnel geometry

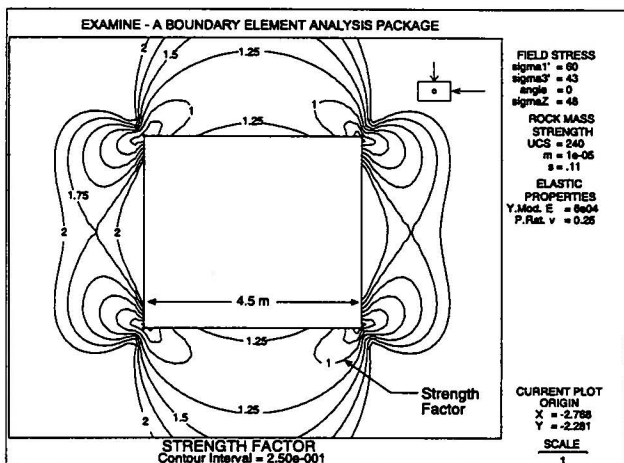
was tried again after excavating without failure using the flat-roof. As soon as the first round was taken with the arched profile, failure occurred.

Fig. 17 shows the predicted depth of failure using the Hoek-Brown frictional parameters expressed as 'Strength Factor' contours for the two geometries in the case history, an arched and a flat-roof tunnel. The Hoek-Brown frictional parameters predicts that the roof of both tunnels will be unstable and that the depth of failure for the flat-roof tunnel will be the greatest.

The same tunnel geometries described above were re-analyzed using Equation 10 and Hoek-Brown brittle parameters (Fig. 18). For this case, only the arched-roof tunnel is predicted to have extensive failure, extending laterally over the entire roof, and radially to a depth of about 1 m. From the analyses, the flat-roof opening should only experience localized failure at



(a) Arched roof



(b) Flat roof

Fig. 18: Depth of failure using the Hoek-Brown brittle failure parameters (Equation 10) for a tunnel with a flat-roof and an arched roof.

the corners and hence would require significantly less support, compared to the tunnel with the arched-roof. This prediction is in keeping with the field observations from the case history, i.e., the flat-roof tunnel is more stable than an arched-roof tunnel, and illustrates that conventional failure criteria are not adequate for estimating the depth of stress-induced brittle failure. Thus for intermediate stress environments, a tunnel with a flat roof is more stable.

However, once in-situ stress magnitudes increase above those used in the case history example, e.g. at depths exceeding 1500 to 2000 m in hard rock, the advantages of the flat roof are diminished. At these higher stress magnitudes the rock mass fails over the entire span of the flat tunnel roof. For these situations the arched roof is more practical as there is less failed

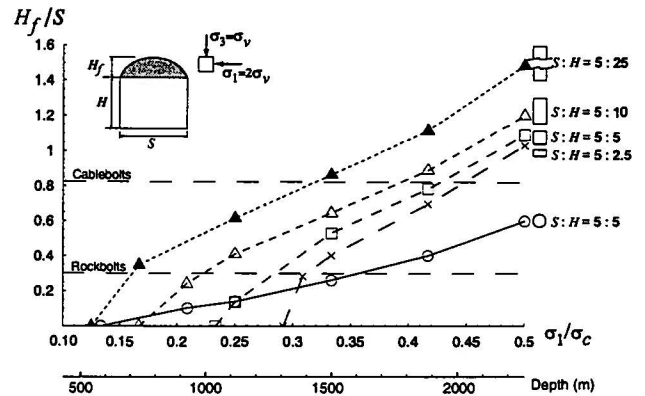


Fig. 19: Depth of brittle failure in the roof of circular and rectangular shaped tunnels.

rock to support. Thus the choice of a flat or arched roof for the tunnel design is significantly influenced by the in-situ or mining-induced stress environment.

5.4 Optimizing tunnel shape for brittle failure

The previous examples illustrated that the shape of the tunnel could be used to control when brittle failure initiates for any given stress state. However in some situations, such as during the excavation of large caverns or openings in a mining environment, the final stress state will change significantly from the original stress state as sequential excavations are used to obtain the final geometry. From a support perspective it is important to know the effect of changing tunnel shape on the depth of brittle failure for various stress states.

A series of Examine2D analyses was carried out to investigate the depth of brittle failure for various shaped openings in a good quality rock mass in the Canadian Shield:

Rock Type	Granite gneiss	
In-situ stress	$\sigma_1 = 2\sigma_3$	
	$\sigma_3 = 0.027 \text{ MPa/m} \times \text{Depth (m)}$	
Intact rock strength	σ_c	240 MPa
Rock Mass Rating	RMR	70
Hoek-Brown constants	m	0
	s	0.11

The analyses used a vertical stress gradient equal to the weight of the overburden and a horizontal stress of twice the vertical stress. This is consistent with general stress trends for the Canadian Shield (Arjang and Herget, 1997). In the analyses, the excavation shapes had a constant span (S) or width of 5 m and a height (H) that varied from 2.5 to 25 m such that the span to height ratios ($S:H$) 0.5, 1, 2 and 5. For all analyses, except the circular shaped tunnel, the geometries had a flat roof.

Fig. 19 shows the results from these analyses in dimensionless form where the depth of brittle failure, measured vertically from the mid-span of the tunnel, is normalized to the span of the opening and the vertical depth of the excavation is expressed

as the ratio of the far-field maximum stress to the unconfined compressive strength, e.g., a depth of 1000 m is expressed as $(1000 \times 0.027 \times 2)/240 = 0.225$. The results show that brittle failure around the circular tunnel initiates at a depth of approximately 500 m ($\sigma_1/\sigma_c \approx 0.12$) and that the increase in the depth of brittle failure is approximately linear as the far-field stress magnitude increases. However, the tunnels with flat-roofs (S:H between 0.5 and 2) show that while the depth of brittle failure initiates at vertical depths far greater than 500 m, the depth of brittle failure quickly increases above that shown by the circular tunnel for a given ratio of σ_1/σ_c . Hence once failure across the roof of the tunnel initiates, the advantages of a flat roof quickly diminish.

In many civil and mining applications support in tunnels with spans less than 5 to 10 m is achieved by the use of fully grouted rockbolts and/or cablebolts. Farmer and Shelton (1980) suggested that for rockbolts, the length (L) of the bolt is related to the span (S) of the opening by:

$$[13] \quad L = 0.3S$$

and Hutchinson and Diederichs (1996) have suggested that the length should be adjusted for cablebolts by adding two metres of embedment length such that the length is related to the span by:

$$[14] \quad L = 0.7S^{0.7} + 2 \text{ m.}$$

These empirical design guidelines for the bolt length as a function of span are indicated in Fig. 19. This figure shows that while rockbolts provide adequate support for brittle failure around a circular tunnel over a wide range of stress to strength ratios their effectiveness is significantly reduced for tunnels with flat roofs, particularly tunnels with span to height ratios greater than 1. Fig. 19 also shows that the extent of brittle failure, for the flat roof tunnels, extends outside the suggested support range of cablebolts at stress to strength ratios greater than about 0.35. Hence for these situations, the arched roof is more practical, as there is less failed rock to support. This example further illustrates that the choice of a flat or arched roof for the tunnel design is significantly influenced by the in-situ stress environment.

6 Conclusions

Empirical evidence indicates that the initiation of stress-induced brittle failure occurs when the damage index, expressed as ratio of the maximum tangential boundary stress to the unconfined compressive strength of the rock mass, exceeds 0.4 ± 0.1 . When this condition occurs the depth of brittle failure around a tunnel in massive to moderately fractured rock can be estimated by using an elastic analysis with the following Hoek-Brown brittle parameters:

$$m = 0 \text{ and } s = 0.11.$$

The fundamental assumption in using these brittle parameters is that the failure process around the tunnel is dominated by

cohesion loss associated with rock mass fracturing. Hence, it is not applicable to conditions where the frictional strength component can be mobilized and dominates the behaviour of the rock mass near the excavation boundary.

The relationship between the damage index and the normalized depth of brittle failure for near circular tunnels is linear. For the depth of brittle failure for non-circular tunnels, when normalized to the span and the far-field stress, it is non-linear. For support design purposes, these relationships can be used to determine the required bolt length and the anticipated gravity loading of the support. The Hoek-Brown brittle parameters can also be used to optimize the shape of openings.

In low-stress environments the arched-shape roof minimizes the region of low confining stresses and hence reduces the potential for structurally-controlled failure. In intermediate-stress environments the flat roof improves roof stability by forcing failure to occur in the corners of the excavation where the confining stress helps to contain the extent of stress-induced fractures. At higher stress magnitudes fracturing extends across the full span of the tunnel roof as the deviatoric stresses exceed $1/3\sigma_c$. For these situations the arched roof is again more favourable as there is less failed rock to support. Thus the choice of a flat or arched roof for the tunnel design depends on the in-situ stress environment.

Acknowledgments

This work was supported by the Natural Sciences and Engineering Research Council of Canada and through collaboration with the hard rock mining industry in Northern Ontario. The authors wish to recognize the contributions made to this work, either directly or through discussions, by Ms. J. Alcott (GRC), Dr. L. Castro (Golder Associates, Inc.), Mr. M. Diederichs (GRC), Ms. S. Espley (Inco Limited), Ms. V. Falmagne (Laurentian University), Dr. R. Read (AECL) and Dr. Xiaoping Yi (GRC).

References

- Arjang, B. and Herget, G., 1997. In situ ground stresses in the Canadian hardrock mines: an update. *International Journal of Rock Mechanics and Mining Sciences*, 34(3-4). Paper No. 015.
- Bieniawski, Z. T., 1989. *Engineering Rock Mass Classifications*. John Wiley & Sons, New York.
- Brace, W. F., Paulding, B., and Scholz, C., 1966. Dilatancy in the fracture of crystalline rocks. *Journal Geophysical Research*, 71: 3939-3953.
- Brady, B. H. G. and Brown, E. T., 1993. *Rock Mechanics for Underground Mining*. Chapman and Hall, London, 2nd edn.
- Brown, E. T., editor, 1981. *Rock Characterization, Testing and Monitoring, ISRM Suggested Methods*. Pergamon Press, Oxford.
- Castro, L. A. M. and McCreath, D. R., 1997. How to enhance the geomechanical design of deep openings. In *Proc. 99th CIM Annual General Meeting, Vancouver*, pp. 1-13, Montreal. Canadian Institute of Mining.
- Castro, L. A. M., McCreath, D. R., and Oliver, P., 1996. Rockmass damage initiation around the Sudbury Neutrino Observatory cavern. In *Proc. 2nd North American Rock Mechanics Symposium*,

- Montreal, edited by M. Aubertin, F. Hassani, and H. Mitri, vol. 2, pp. 1589–1595, Rotterdam. A.A. Balkema.
- Curran, J. H. and Corkum, B. T., 1995. Examine^{2D}—A 2D boundary element program for calculating stresses around underground excavations in rock, Version 5. Rock Engineering Group, University of Toronto, Toronto, Canada.
- Curran, J. H. and Corkum, B. T., 1997. Phase²—A 2D plastic-finite element program for calculating stresses and estimating support around underground excavations, Version 1. Rock Engineering Group, University of Toronto, Toronto, Canada.
- Detournay, E. and St. John, C. M., 1988. Design charts for a deep circular tunnel under non-uniform loading. *Rock Mechanics and Rock Engineering*, 21(2): 119–137.
- Fairhurst, C., 1993. Analysis and design in rock mechanics—The general context. In *Comprehensive Rock Engineering – Rock Testing and Site Characterization*, edited by J. A. Hudson, vol. 2, pp. 1–29. Pergamon Press, Oxford.
- Fairhurst, C. and Cook, N. G. W., 1966. The phenomenon of rock splitting parallel to the direction of maximum compression in the neighbourhood of a surface. In *Proc. of the 1st Congress of the International Society of Rock Mechanics*, Lisbon, pp. 687–692.
- Farmer, I. W. and Shelton, P. D., 1980. Factors that affect underground rockbolt reinforcement systems. *Transactions of the Institution of Mining and Metallurgy (Section A: Mining Industry)*, 89: A68–A83.
- Greenspan, M., 1944. Effect of a small hole on the stresses in a uniformly loaded plate. *Quarterly Applied Math*, 2(1): 60–71.
- Grimstad, E. and Bhasin, R., 1997. Rock support in hard rock tunnels under high stress. In *Proc. Int. Symp. on Rock Support—Applied Solutions for Underground Structures*, Lillehammer, edited by E. Broch, A. Myrvang, and G. Stjern, pp. 504–513. Norwegian Society of Chartered Engineers, Oslo.
- Hallbauer, D. K., Wagner, H., and Cook, N. G. W., 1973. Some observations concerning the microscopic and mechanical behaviour of quartzite specimens in stiff, triaxial compression tests. *International Journal of Rock Mechanics Mining Science & Geomechanics Abstracts*, 10: 713–726.
- Hoek, E. and Brown, E. T., 1980. *Underground Excavations in Rock*. The Institution of Mining and Metallurgy, London.
- Hoek, E. and Brown, E. T., 1988. The Hoek-Brown failure criterion - a 1988 update. In *Proc. 15th Canadian Rock Mechanics Symposium*, Toronto, edited by J. H. Curran, pp. 31–38. Department of Civil Engineering, University of Toronto, Toronto.
- Hoek, E., Kaiser, P. K., and Bawden, W. F., 1995. *Support of Underground Excavations in Hard Rock*. A. A. Balkema, Rotterdam.
- Hutchinson, D. J. and Diederichs, M. S., 1996. *Cablebolting in Underground Mines*. BiTech Publishers Ltd., Richmond.
- Jiayou, L., Lihui, D., Chengjie, Z., and Zebin, W., 1989. The brittle failure of rock around underground openings. In *Proc. Conf. on Rock Mech. and Rock Physics at Great Depth*, Pau, France, edited by V. Maury and D. Fourmaintraux, vol. 2, pp. 567–574. A.A. Balkema, Rotterdam.
- Kirsten, H. A. D. and Klokow, J. W., 1979. Control of fracturing in mine rock passes. In *Proc. 4th, ISRM Congress on Rock Mechanics*, Montreux, vol. 1, pp. 203–210, Rotterdam. A. A. Balkema.
- Martin, C. D., 1989. Failure observations and in situ stress domains at the Underground Research Laboratory. In *Proc. Conf. on Rock Mech. and Rock Physics at Great Depth*, Pau, France, edited by V. Maury and D. Fourmaintraux, vol. 2, pp. 719–726. A.A. Balkema, Rotterdam.
- Martin, C. D., 1995. Brittle rock strength and failure: Laboratory and in situ. In *Proc. 8th, ISRM Congress on Rock Mechanics*, Tokyo, edited by T. Fujii, vol. 3, pp. 1033–1040, Rotterdam. A.A. Balkema.
- Martin, C. D., 1997. Seventeenth Canadian Geotechnical Colloquium: The effect of cohesion loss and stress path on brittle rock strength. *Canadian Geotechnical Journal*, 34(5): 698–725.
- Martin, C. D. and Chandler, N. A., 1994. The progressive fracture of Lac du Bonnet granite. *International Journal of Rock Mechanics Mining Science & Geomechanics Abstracts*, 31(6): 643–659.
- Martin, C. D., Martino, J. B., and Dzik, E. J., 1994. Comparison of borehole breakouts from laboratory and field tests. In *Proc. EU-ROCK'94, SPE/ISRM Rock Mechanics in Petroleum Engineering*, Delft, pp. 183–190, Rotterdam. A.A. Balkema.
- Martin, C. D., Read, R. S., and Martino, J. B., 1997. Observations of brittle failure around a circular test tunnel. *International Journal of Rock Mechanics and Mining Sciences*, 34(7): 1065–1073.
- Martin, C. D., Young, R. P., and Collins, D. S., 1995. Monitoring progressive failure around a tunnel in massive granite. In *Proc. 8th, ISRM Congress on Rock Mechanics*, Tokyo, edited by T. Fujii, vol. 2, pp. 627–633, Rotterdam. A.A. Balkema.
- Myrvang, A. M., 1991. Estimation of in situ compressive strength of rocks from in situ stress measurements in highly stressed rock structures. In *Proc. 7th ISRM Congress on Rock mechanics*, Aachen, edited by W. Witke, pp. 573–575. A.A. Balkema, Rotterdam.
- Nickson, S., Spratt, D., Bawden, W. F., and Coulson, A., 1997. A geomechanical study for a shaft wall rehabilitation program. In *Proc. 99th CIM Annual General Meeting*, Vancouver, pp. 1–20, Montreal. Canadian Institute of Mining.
- Ortlepp, W. D., 1997. *Rock Fracture and Rockbursts – An Illustrative Study*. Monograph Series M9. The South African Institute of Mining and Metallurgy, Johannesburg.
- Ortlepp, W. D. and Gay, N. C., 1984. Performance of an experimental tunnel subjected to stresses ranging from 50 MPa to 230 MPa. In *Proc. ISRM Symp.: Design and Performance of Underground Excavations*, edited by E. T. Brown and J. Hudson, pp. 337–346. British Geotechnical Society, London.
- Ortlepp, W. D., O'Ferral, R. C., and Wilson, J. W., 1972. Support methods in tunnels. *Association of Mine Managers of South Africa. Papers and Discussion*, pp. 167–195.
- Pelli, F., Kaiser, P. K., and Morgenstern, N. R., 1991. An interpretation of ground movements recorded during construction of the Donkin-Morion tunnel. *Canadian Geotechnical Journal*, 28(2): 239–254.
- Peng, S. S. and Johnson, A. M., 1972. Crack growth and faulting in cylindrical specimens of Chelmsford granite. *International Journal of Rock Mechanics Mining Science & Geomechanics Abstracts*, 9: 37–86.
- Read, R. S. and Chandler, N. A., 1997. Minimizing excavation damage through tunnel design in adverse stress conditions. In *Proceedings of the International Tunnelling Association World Tunnel Congress*, Vienna, vol. 1, pp. 23–28, Rotterdam. A.A. Balkema.
- Read, R. S. and Martin, C. D., 1996. Technical summary of AECL's Mine-by Experiment Phase 1: Excavation response. *AECL Report AECL-11311*, Atomic Energy of Canada Limited.
- Sakurai, S., 1993. Back analysis in rock engineering. In *Comprehensive Rock Engineering - Excavation, Support and Monitoring*, edited by J. A. Hudson, vol. 4, pp. 543–569. Pergamon Press, Oxford.
- Scholz, C. H., 1968. Microfracturing and the inelastic deformation of rock in compression. *Journal Geophysical Research*, 73(4): 1417–1432.

- Stacey, T. and Page, C. H., 1986. Practical Handbook for Underground Rock Mechanics, vol. 12 of Series on Rock and Soil Mechanics. Trans Tech Publications, Clausthal-Zerrefeld, Germany.
- Stacey, T. R., 1981. A simple extension strain criterion for fracture of brittle rock. *International Journal of Rock Mechanics Mining Science & Geomechanics Abstracts*, 18: 469–474.
- Stacey, T. R. and de Jongh, C. L., 1977. Stress fracturing around a deep-level bored tunnel. *Journal of the South African Institute of Mining and Metallurgy*, pp. 124–133.
- Wagner, H., 1987. Design and support of underground excavations in highly stressed rock. In *Proc. 6th ISRM Int. Congress on Rock Mechanics*, Montreal, edited by G. Herget and S. Vongpaisal, vol. 3, pp. 1443–1457. A.A. Balkema, Netherlands.
- Wiseman, N., 1979. Factors affecting the design and condition of mine tunnels. *Research Report 45/79*, Chamber of Mines of South Africa, Pretoria, South Africa.